

# Modelling the onset of oxide formation on metal surfaces from first principles

Lucio Colombi Ciacchi

*Fraunhofer Institut für Werkstoffmechanik IWM,*

*Freiburg, Germany, and*

*Institut für Zuverlässigkeit von Bauteilen und Systemen,*

*Universität Karlsruhe, Karlsruhe, Germany.*

The formation of ultrathin oxide layers on metal surfaces is a non-thermally-activated process which takes place spontaneously at very low temperatures within nanoseconds. This paper reports mechanistic details of the initial oxidation of bare metal surfaces, in particular Al(111) and TiN(001), as obtained by means of first-principles molecular dynamics modelling within the Density-Functional Theory. It is shown that the reactions of bare metal surfaces with O<sub>2</sub> molecules take place according to a “hot-atom” dissociative mechanism which is triggered by the filling of the  $\sigma^*$  antibonding molecular orbital and is characterised by a sudden release of a large amount of kinetic energy. This released energy provides a driving force for metal/oxygen place-exchange processes which are responsible for the onset of oxide formation at virtually 0 K and at oxygen coverages well below 1 monolayer (ML). Further simulations of the oxidation reactions reveal that a disordered ultrathin oxide forms on Al(111), whereas a rather ordered structure develops on TiN(001) following a selective oxidation process which leaves clusters of Ti vacancies in the TiN lattice underneath the oxide layer.

# 1. Introduction

Metal surfaces in contact with the atmosphere become quickly covered by oxide layers of thicknesses which vary from few atomic layers (less than 1 nm) to several microns, depending on the reactivity of the metal and the history of the sample [1]. Even the noblest metals, such as gold, may chemically interact with oxygen species [2] at their surfaces. The oxide skin governs the chemical and physical interactions of the metal with the outer environment, thus a precise knowledge of its structure and composition is fundamental to a number of technologically important problems. These comprise for instance the behaviour of metallic biomedical implants within the chemically aggressive physiological environment [3], the response of electrodes or sensors in direct contact with liquid solutions [4,5], the performances of metallic contact structures in electronic devices, the wear and friction properties of metal surfaces [6], the rate of sub-critical crack propagation due to stress-corrosion phenomena [7], and many others [8].

Traditionally, engineers have been much concerned with oxidation phenomena at high temperatures, since they result in a continuous consumption of metal and therefore inevitably limit the life of machine components such as, for instance, turbine blades [1]. For this reason, great effort has been expended in the last century to develop a basic understanding of the kinetic laws governing high-temperature oxidation, and several theories have been formulated which explain and predict the oxidation behaviour of many metals and metal alloys [9–11]. However, as noted in [1], many of the existing rate laws seem to be satisfactory only over a limited oxide thickness range, and often are not transferable to low temperature or low pressure regimes.

In particular, detailed knowledge of processes of oxide formation at room temperature or below is scarce compared with the amount of information available in the field of high-temperature oxidation. The available kinetic models rely on assumptions on the nature of characteristic defects in the formed oxide, which govern the diffusion processes necessary to oxide growth [12,13]. In turn, this requires a precise knowledge of the structure and composition of the ultrathin oxide layers which form spontaneously

when a bare surface is put in contact with an oxidising environment. These layers are often glassy oxides of non-integer stoichiometry, so structural information on the oxide lattice or on the defects present cannot be inferred from the corresponding bulk oxide structures which form at more elevated temperatures or oxygen pressures [14]. Moreover, in the case of ultrathin oxide layers it is very difficult, if not impossible, to define a precise metal/oxide interface as in the case of thicker crystalline oxides grown on metals (see e.g. [15,16]).

Differently to the growth of oxide layers at high temperature, which is limited basically by the thermally activated diffusion of ionic species across the oxide layer, the initial reactions of a bare metal surface with an oxidising atmosphere are not thermally activated. Namely, spontaneous formation of a few monolayers of oxide has been observed at temperatures as low as a few K [17,18]. Formation of an oxide layer takes place if adsorbed oxygen atoms can change place with underlying metal atoms and be incorporated below the metal surface. Driving forces for this metal/oxygen place-exchange process are in principle available due to the generally high heat of adsorption of oxygen on metals, and due to the large electric field which develops at the metal/oxide interface as a consequence of electron donation from the metal to the incoming oxygen [10,11]. However, the mechanistic details of the actual exchange process are still unknown, and it remains to be understood how this can take place at virtually 0 K [6].

Our goal is to gain a mechanistic insight into the events of initial oxide formation on metal surfaces, prior to the beginning of a diffusion-limited oxide growth process. As these events are not thermally activated and occur on a scale of picoseconds to nanoseconds, they are hardly accessible through commonly available experimental techniques. Therefore, they will be addressed in this work by means of “first-principles” atomistic modelling at the quantum mechanical level [19]. Helped by the fast development of accurate and efficient theoretical formalisms and by the ever-increasing power of computer platforms, this is becoming one of the methods of choice to investigate chemical processes in materials science at the atomic scale [20]. In particular, so-called first-

principles thermodynamics approaches have been widely used in the last few years to address the structure and composition of thin oxide layers on metal surfaces (see e.g. [14,21,22]). Such approaches give precise information on the different oxide phases and structures which are thermodynamically stable at various temperatures and oxygen pressures. However, low-temperature oxidation reactions may lead to formation of intrinsically metastable, often amorphous, oxide structures. Therefore, here we will investigate their formation via a first-principles molecular dynamics approach. This technique is obviously limited by the small system size and the short simulation time addressable, but provide us with a detailed information on the dynamical features of the oxidation reactions which would be very difficult to gain otherwise. Moreover, using molecular dynamics we are able to obtain structural models of metastable glassy oxide layers which may capture the physical and chemical properties of ultrathin oxide layers formed at low temperatures more realistically than the corresponding thermodynamically stable phases. The growth of oxide scales of larger thickness can be simulated using atomistic techniques at the classical level, which, however, necessarily need to be tuned on previous knowledge from unbiased simulations at the quantum level [23,24].

## 2. Computational details

All the results presented in the following sections were obtained using molecular dynamics techniques in which the forces acting on the atoms are computed within the Density-Functional Theory (DFT) quantum mechanical formalism. Using a first-principles approach, as comprehensively reviewed in [19,20,25,26], is strictly necessary to investigate processes involving creation and rupture of covalent bonds. After computing the forces within the DFT, the atoms are moved according to the classical equation of motion integrated with standard algorithms [27]. All the calculations in the present work were carried out in this theoretical framework, using the LAUTREC code [28]. Both the minimisation of the electronic states and the dynamics of the atoms were performed using the Car–Parrinello (CP) method [29] and the gradient-corrected exchange-correlation

potential PW91 [30]. Either separable, norm-conserving atomic pseudopotentials [31] or Blöchl’s Projector Augmented Waves approach [32] have been used to describe the electron–nucleus interactions including in the simulations only the valence electrons. The CP simulations of metallic systems were performed with the algorithm proposed in Refs. [33] and [34]. The simulated systems are periodically repeated in all directions of space. Surface models were constructed including in the simulation cell a slab of a few layers of metal atoms separated from its periodically repeated image by a vacuum layer in the direction perpendicular to the surface. The thickness of the slab and of the vacuum layer have been chosen so as to avoid spurious effects due to truncation of the crystal or interactions with the image systems. Details of the simulation parameters and test calculations to assess the precision of the formalism can be found, in particular, in [3, 35, 36].

### 3. O<sub>2</sub> adsorption on bare metal surfaces

#### 3.1. Experimental background

Bare metal or semiconductor surfaces are intrinsically very reactive systems. The cleavage of a crystal along a given crystallographic direction leaves under-coordinated surface atoms and broken, “dangling” bonds which readily participate in chemical reactions with molecules in proximity of the surface. A pictorial representation of the dangling bonds of a Si(001) surface is given in Fig. 1 (top), where the computed Electron Localisation Function (ELF) [37] of the system is depicted as a green iso-surface. Regions of large ELF far from the atomic cores and of chemical bonds are indicative of the presence of lone electrons, and thus of potentially reactive sites for chemical reactions. In fact, any Si surface put in contact with the atmosphere at normal temperature and pressure conditions would promptly react with dioxygen and water molecules and become covered by an amorphous ultrathin hydroxylated oxide layer within a few nanoseconds (Fig. 1, bottom). Metal surfaces behave in the same

way, although the electrons available for donation into oxidising molecules are rather uniformly delocalised over the atoms composing the surface.

The reactions between  $\text{O}_2$  molecules and bare metal surfaces have been studied using scanning tunneling microscopy (STM) under ultrahigh vacuum conditions [38–40]. When a previously cleaned metal surface is treated with a flow of oxygen gas at low pressure, pairs of oxygen atoms separated by distances of about 1 to 3 nearest-neighbour metal–metal distances become visible under the STM (Fig. 2). This suggests that  $\text{O}_2$  reacts dissociatively with metal surfaces by cleavage of the O–O bond, leading to pairs of single adsorbed oxygen atoms. On the Al(111) surface at room temperature or below, the reaction may proceed with adsorption of only one O atom and ejection of the second O atom in the gas-phase [40]. This process is still thermodynamically favoured since the heat of adsorption of just a single atom on Al(111) is more than 7 eV, while the energy required to break the O–O bond of  $\text{O}_2$  is slightly larger than 5 eV. Both the possibility of O ejection and the large distances (up to  $\sim 10$  Å) which separate pairs of atoms after the oxidation reaction at very low temperatures indicate that the dissociation process of  $\text{O}_2$  on the metal surface is associated with a sudden release of high kinetic energy. This energy release enables the atoms to overcome relatively large diffusion barriers over the surface (of the order of  $\sim 0.5$  eV) and to cover distances much larger than a normal thermally activated diffusion process would allow at the low reaction temperatures. Therefore, the term “hot-atom”-mechanism has been used in the literature to describe the non-thermally-activated process of dioxygen dissociation on metals [38, 41].

In the following section, first-principles molecular dynamics (FPMD) simulations of the process of dioxygen dissociation on several metal surfaces will be reported, focusing on the actual driving force for the occurring “hot-atom” dissociation event.

### 3.2. “Hot-atom” dissociation of O<sub>2</sub> on bare metal surfaces

Before describing the results of FPMD simulations of the dissociative adsorption of dioxygen on metallic surfaces, it is useful to summarise very briefly some features of the molecular orbitals of O<sub>2</sub> (Fig. 3). Dioxygen is a paramagnetic molecule, having the two degenerate  $\pi^*$  antibonding orbitals each filled with one electron of equal spin. The empty  $\sigma^*$  orbital lies almost 7 eV higher in energy than the  $\pi^*$  orbitals, and the  $p_x$  orbital lobes along the direction of the O–O bond are evidently compressed in the interatomic bond region (see Fig. 3, right). It needs to be noted that within our ground state DFT method we are not able to address excited electronic states of dioxygen, which may in principle have a role in the oxidation reactions. However, as discussed in [35], the mechanisms of onset of oxide formation are expected not to be influenced qualitatively by the adiabaticity of the DFT simulations.

The adsorption of an O<sub>2</sub> molecule on the Al(111) surface has been simulated using a periodically repeated surface slab of five (111) atomic layers separated by a vacuum layer of the same thickness (Fig. 4). When an oxygen molecule is placed near this surface slab, the two unpaired electrons in the  $\pi^*$  molecular orbitals can be visualised by imaging of the spin-density of the system. This is defined as the difference  $\Delta\rho$  between the particle densities  $\rho_\alpha$  and  $\rho_\beta$  associated with each spin-manifold. In Fig. 4a, the O–O axis of the oxygen molecule is perpendicular to the plane of the page, and the radial symmetry of the  $\pi^*$  antibonding orbitals is evident. When the molecule is about 3.0 Å above the surface, the integrated spin density is about 1.8 electrons, indicating a partial charge donation from the surface into the molecule, and thus a chemical interaction between molecule and surface. This is also revealed by analysis of the local density of states (LDOS) integrated within spheres around the O atoms with radii corresponding to the covalent radius of oxygen (Fig. 5). Namely, the lower edge of the LUMO orbital of dioxygen is placed at the Fermi level of the system (Fig. 5, top) so that the orbital is not completely empty. As a general shortcoming of standard DFT techniques, the barrier for passing from a physisorbed molecular state to a chemically

adsorbed (and dissociated) state on the Al surface is missing (for a thorough discussion of this issue, see e.g. [42]).

Indeed, after starting the dynamics, the molecule is quickly adsorbed on the surface in a process which is characterised by a full quenching of the spin density due to electron donation into the half-filled  $\pi^*$  antibonding orbital of  $\text{O}_2$  (Fig. 4b, c and Fig. 5, middle). This leads to a gradual increase of the O-O distance, until also the  $\sigma^*$  antibonding orbital of the adsorbed molecule becomes partially populated, as revealed by analysis of the spin density (Fig. 4d) and of the LDOS (Fig. 5, bottom). The O-O bond dissociates as a consequence of this event, the O-O distance increasing abruptly in a way which is indicative of a non-thermal, “hot-atom” mechanism (Fig. 4e, f). The sudden release of kinetic energy during the dissociation is large enough to push one of the O atoms below the Al surface, while one Al atom is pulled out of the surface (Fig. 4e). However, in the subsequent dynamics the O atom emerges again above the surface and the gained kinetic energy is gradually transferred via the lattice vibrations to the whole surface slab. After quenching of the atomic motion, the O atoms are stably adsorbed in hollow surface sites, separated by a distance of 5.9 Å, i.e. by more than two Al-Al distances.

In a number of similar FPMD simulations, the same “hot-atom” dissociation mechanism has been observed to lead to spontaneous  $\text{O}_2$  dissociation on Al(100), Ti(0001), Co(0001), Cr(110), TiN(001), and notably also on Si(001) [36]. We may thus consider it as a general mechanism for the initial reaction of dioxygen molecules with bare metal or semiconductor surfaces. Among the system investigated so far, only the reaction of dioxygen with Pt(111) resulted in stable adsorption of molecular  $\text{O}_2$  without dissociation. In fact, the experimental evidence is that dissociation of  $\text{O}_2$  on Pt(111) occurs only at temperatures higher than  $\sim 150$  K [41], while our simulations are all performed starting from fully relaxed systems, i.e. at virtually 0 K. However, when dissociation is observed experimentally, then the process bears all the typical features of a “hot-atom” mechanism [41]. This suggests that thermal motion of the surface is necessary to activate the  $\text{O}_2$  molecule so that the O-O distance becomes sufficiently



large to enable partial filling of the  $\sigma^*$  antibonding molecular orbital. After that, we expect the dissociation to proceed similarly to all other cases considered.

The dynamical evolution of an  $\text{O}_2$  molecule during a FPMD simulation of its adsorption and dissociation on the  $\text{Al}(100)$  surface is reported in Fig. 6. In the top graph the evolution of the intramolecular O–O distance is plotted together with the evolution of the distance between the centre of mass of the two O atoms and the surface. The bottom graph reports the evolution of the spin density and the charge on the atoms integrated within the Bader regions [43] associated with both O atoms. It is interesting to note that after the initial adsorption of the molecule on the surface (left vertical dotted line), the charge on the molecule is only slightly more than 1.0 electron. Only as a consequence of the “hot-atom” dissociation event (right vertical dotted line), which suddenly cleaves the molecular bond, do the O atoms become charged each with almost two electrons. This highlights the fact that the hyperthermal dissociation is not triggered by Coulomb repulsion between the O atoms, but by the Pauli repulsion between the partially occupied p-type orbitals along the O–O axis [35].

## 4. Spontaneous formation of ultrathin oxide layers

### 4.1. Onset of oxide formation at increasing oxygen coverages

The same technique used to simulate the adsorption of single oxygen molecules on bare surfaces has been applied to investigate further oxidation reactions at increasing coverages of adsorbed oxygen on the  $\text{Al}(111)$ ,  $\text{Ti}(0001)$  and  $\text{TiN}(001)$  surfaces. Namely, for each system, consecutive FPMD simulations of the adsorption of oxygen molecules have been performed starting with a new  $\text{O}_2$  molecule about 3.0 Å above the relaxed surface obtained in the previous simulation. On both  $\text{Al}(111)$  and  $\text{Ti}(0001)$ ,  $\text{O}_2$  is again observed to adsorb and dissociate spontaneously with a sudden release of kinetic energy. Interestingly, in both systems the process lead to incorporation of O atoms underneath the surface layer at a coverage of 0.50 ML. At this coverage, on  $\text{Al}(111)$  an

Al vacancy is created temporarily as a consequence of the “hot-atom”  $\text{O}_2$  dissociation, and is quickly filled by a previously adsorbed O atom nearby (Fig. 7, left). This process represents the onset of formation of an oxide phase, as pointed out in Ref. [44]. The fact that this is observed in our simulation at a coverage well below the saturation of one  $(1\times 1)$  O adlayer is indeed consistent with the experimental finding that oxide nucleation can start at coverages as low as 0.2 ML [44]. A similar scenario is observed on Ti(0001), where the motion of the surface Ti atoms induced by the energy released upon dissociation is such that a previously adsorbed O atom is able to penetrate the surface layer and bind to the Ti layer underneath (Fig. 7, middle). These simulations strongly suggest that place-exchange processes between metal atoms and O atoms are spontaneously activated during the oxidation reaction due to the high kinetic energy associated with the cleavage of the O–O bond of incoming  $\text{O}_2$  molecules.

Interestingly, such place-exchange mechanisms are not observed in simulations of oxidation reactions on the TiN(001) surface at low oxygen coverages. In this case, no O atoms are incorporated underneath the surface, whereas Ti atoms are observed to escape from the topmost surface layer (Fig. 7, right) and bind to the incoming oxygen. Also, not all  $\text{O}_2$  molecules are observed to dissociate spontaneously, indicating a decreased reactivity of the partially oxidised surface with respect to the bare TiN surface. In particular, increasing the simulation temperature to 600 K was not sufficient to dissociate the molecule depicted in Fig. 7(right) within 2.5 ps of simulation time.

## 4.2. Formation of ultrathin oxide layers

Further FPMD simulations of reactions with  $\text{O}_2$  molecules with the partially oxidised Al(111) and TiN(001) surfaces were performed to increase the oxygen coverage beyond the onset of oxide formation described in the previous section. These are described separately for each system in the following two subsections.

### Formation of amorphous oxide on Al(111)

On Al(111) further reactions with dioxygen proceeded spontaneously at virtually 0 K (i.e., both the surface and the molecules were fully relaxed in the initial configuration of each FPMD run) up to a coverage of 1.0 ML [35]. After that, O<sub>2</sub> molecules initially placed at a distance of about 3.0 Å above the surface were repelled by the already formed ultrathin oxide structure. Therefore, O<sub>2</sub> molecules were placed in close contact with Al atoms at potentially reactive sites on the outer oxide surface (the initial Al–O distances were about 2.0 to 2.5 Å). Although some of the molecules were again repelled by the surface and desorbed, in a few cases spontaneous dissociation took place, leading to growth of the oxide layer up to a coverage of 1.5 ML. The final structure obtained is reported in Fig. 8. Noteworthy is the evident disorder in the oxide structure along the direction perpendicular to the surface, while a top-view (bottom left in Fig. 8) reveals a certain order in the surface plane, in which the O atoms are arranged in positions roughly correspondent to the hollow sites of the Al(111) plane. Also interesting is the fact that the initially formed oxide structure presents large cavities at the metal/oxide interface, which seem to be consistent with the low density of the thin amorphous oxide on Al(111) observed in x-ray photoelectron spectroscopy (XPS) experiments [45]. In fact, the XPS evidence suggests that only after reaching a critical thickness does the oxide layer undergo a transition to a crystalline state, which is associated with a densification of the oxide layer [45].

It needs to be stressed that the dynamics of the spontaneous reactions described above, and in particular the occurrence of metal/oxygen place-exchange processes after dissociative adsorption of O<sub>2</sub> molecules, does lead to oxide structures which are not necessarily in thermodynamical equilibrium. This is evident by looking at the computed total energy per unit cell of the oxidised Al(111) surface at an oxygen coverage of 1 ML (the unit cell contains 60 Al atoms and 12 O atoms). The energy of the disordered structure obtained after consecutive FPMD simulations is  $\sim 3$  eV higher than the energy of an ordered monolayer of adsorbed O atoms on fcc surface sites. However, the

energy released after the oxidation reactions is very quickly dissipated to vibrational modes of the underlying Al lattice, so that the formed disordered structure is not able to rearrange back into an ordered ad-layer of oxygen atoms. Moreover, the metal/oxygen place-exchange processes are favourable from an electrostatic point of view, since they lead to a decrease in the surface dipole which develops as a consequence of donation of electronic charge from the metal to the adsorbed oxygen. This can be quantified by computing the increase of the work function of the metal surface upon oxidation. This increases by 0.32 eV in the case of the spontaneously formed oxide structure and by 0.46 eV in the case of the ordered O adlayer. Therefore, a rearrangement of the formed disordered structure to an ordered adlayer requires not only thermal activation to overcome the diffusion barriers, but an additional activation energy due to the unfavourable electrostatics. In conclusion, we expect such rearrangements not to take place at room temperature or below, while they are certainly not excluded at higher oxidation temperatures (at which, however, other ordered ultrathin oxide structures may become thermodynamically favourable with respect to an O adlayer [46]).

#### Formation of ordered oxide on TiN(001)

The final snapshots of six consecutive FPMD simulations of the initial oxidation of a TiN(001) surface model containing 9 Ti and 9 N atoms in the periodically repeated simulation surface cell are reported in Fig. 9. As outlined above, the initial reactions of O<sub>2</sub> molecules with the TiN(001) surface take place without incorporation of O atoms underneath the surface. Instead, Ti atoms are observed to escape the surface plane to become coordinated by the incoming oxygen atoms, leaving behind Ti vacancies in the TiN lattice (Fig. 9b–e). In this process, the surface Ti atoms leave their coordination shell of five nitrogen atoms as a consequence of their exceedingly high formal oxidation state when oxygen atoms are adsorbed on the surface [3]. The process can also be understood in terms of an increase of the ionic character of the Ti–N bonds leading to their destabilisation after the formation of the Ti–O bonds [47]. Therefore, the initial oxide formation on TiN appears to be driven by a chemical driving force which induce

the formation of a mixed-valence  $\text{TiN}_x\text{O}_y$  surface phase [3].

In many of the simulations, dioxygen dissociation did not occur spontaneously, so that  $\text{O}_2$  molecules remained stably adsorbed on the partially oxidised surface for the entirety of the simulation runs. In the last simulation, the temperature was gradually increased to about 600 K within the first 2 ps of simulated time, then the system was annealed at this temperature for about 2 ps. Subsequently the temperature was gradually increased to about 900 K within 1 ps and the system annealed for about 4 ps before quenching the atomic motion and fully minimising the atomic position. An interesting feature observed during this simulation is the diffusion of Ti vacancies to the second atomic layer below the surface and the creation of Ti interstitials between the first and second Ti layers and at the metal/oxide interface. Moreover, the vacancies created seem to have a tendency to cluster together, as can be seen in Fig. 10 where the final structure obtained is reported showing two periodically repeated simulation cells. Clustering of vacancies at the metal/oxide interface has been indeed observed experimentally upon selective Al oxidation of an intermetallic TiAl surface [48].

During the dynamics, the initially present  $\text{O}_2$  molecules dissociated and the oxide structure underwent a profound rearrangement to form an infinite chain of fourfold-coordinated Ti atoms (Fig. 10) above the existing oxide layer. This structure resembles very closely the proposed “ad-molecule” reconstruction of anatase  $\text{TiO}_2(001)$  [49]. Other Ti atoms remained in a fivefold coordination (being bound both to oxygen atoms and to nitrogen atoms of the substrate), as commonly found on titanium dioxide surfaces, such as, e.g. rutile  $\text{TiO}_2(110)$  [50]. The ordering achieved in the final structure is remarkable given the short simulation time accessible to our technique. It is probably due to the strict matching conditions imposed by the underlying TiN lattice, on which O atoms can only bound to Ti sites, and Ti atoms only to N sites. Notably, at this stage it is already possible to identify three chemically different Ti species. Namely, (i) the fourfold-coordinated Ti atoms bound to only oxygen, (ii) the Ti atoms at the interface bound to both oxygen and nitrogen, and (iii) the Ti atoms of the bulk bound to only nitrogen atoms. These three chemical species are indeed typically found in

XPS investigations of the oxide layers grown on TiN substrates [3, 47, 51].

Finally, it is to be noted that in spite of the profound rearrangements of the oxide layer formed, the N atoms of the TiN lattice remained in their equilibrium positions. Therefore, formation of thicker  $\text{TiO}_2$  layer and release of gaseous  $\text{N}_2$  are expected to involve a slower, activated process. This may be consistent with a number of XPS experiments where  $\text{TiN}_x\text{O}_y$  compounds have been observed to form uniformly over the entire region of a TiN film in the early oxidation stages, prior to the formation of an amorphous  $\text{TiO}_2$  layer. This is then converted into a crystalline  $\text{TiO}_2$  film only after a thermal treatment at higher temperatures [47, 51]. Moreover, the native oxide layer formed at room temperature has been found to be substantially thinner on TiN than on Ti [51], which reflects the high stability of the  $\text{TiN}_x\text{O}_y$  surface phase.

## 5. Conclusions and outlook

Despite evident differences among the systems investigated, all our FPMD simulations indicate that the onset of oxide formation on metal surfaces at low temperature is driven by the kinetic energy released during the dissociative adsorption of  $\text{O}_2$  molecules. After the single reactions, the oxide structures obtained become quickly frozen into a metastable state due to energy dissipation via lattice vibration before the next molecular reaction can take place. In fact, the rate of collision  $r$  of a molecular gas with a solid surface is:

$$r = \frac{p}{\sqrt{2\pi M k_B T}}, \quad (1)$$

where  $M$  is the molecular mass,  $k_B$  the Boltzmann constant,  $T$  the absolute temperature and  $p$  the gas pressure. From this it follows that at a pressure of 1 atmosphere and a temperature of 300 K,  $1 \text{ nm}^2$  of metal surface would be hit by about 3 oxygen molecules every nanosecond. This justifies our choice of quenching the atomic motion at the end of each simulation (lasting no more than 10 ps) and starting the next consecutive simulation of  $\text{O}_2$  adsorption from fully minimised atomic positions.

Provided that all molecular collisions lead to dissociative oxygen adsorption, as can be indeed observed on many metal surfaces, this would lead to formation of a monolayer of oxide within 2 to 3 ns. Only after formation of a few ML of oxide does the probability of reaction with further oxygen molecules rapidly decrease, in a way which is strongly dependent on the metal considered [8]. The case of Al(111) is a peculiar one, since the fraction of oxygen molecules which actually react upon collision (the so-called sticking coefficient) is relatively low ( $10^{-3}$  to  $10^{-2}$ ) at very low oxygen coverages [52]. Therefore, an ultrathin oxide layer on Al(111) is expected to form in less than a microsecond under normal atmospheric conditions.

The emerging scenario is one in which surfaces exposed to an oxidising atmosphere become almost instantaneously covered by an ultrathin oxide layer whose structure and composition may not represent the thermodynamical equilibrium situation. However, this does not mean that amorphous thin oxide layers are necessarily metastable with respect to the corresponding crystalline phases. As outlined in [13, 53], factors such as lattice mismatch, stress in the oxide layer, formation of dislocations at the metal/oxide interface etc. will have a strong influence on the actual stability of the oxides formed. At the level of the simulations described in this work, the formation of vacancies and their clustering underneath the oxide layer may have a direct influence on the stability and on the physical properties of the native oxide layers. This is an issue of particular importance during the formation of native oxides on alloys via the selective oxidation of only one element present in the alloy, and will be the subject of future investigations.

Another factor that should be taken into account is the presence of water vapour in the atmosphere at normal conditions, which may condensate as a thin film on oxidised metal surfaces. Water has been observed indeed to readily react dissociatively with an oxidised Si(001) surface in FPMD simulations [54]. Thus, in general the oxide layer will be terminated by an amount of hydroxyl groups, similarly to what is shown in the bottom panel of Fig. 1.

Our future efforts will be directed at obtaining models of native oxide layers on technological metal surfaces capturing their chemical and physical properties under normal

atmospheric conditions in a possibly realistic way. Knowing the essential details of the structure, composition and electronic structure of native oxide layers may then enable us to construct analytic potentials to study the interactions between oxidised surfaces and the external environment at the classical simulation level, or within hybrid quantum/classical formalisms. This will certainly be necessary in order to address processes which occur on larger size and time scales than what is within the reach of purely quantum mechanical schemes. A prototypical example would be the initial adsorption on metal surfaces of proteins which mediate the interactions between biomedical implants and living cells, just to name a field which is of particular interest both to the author and to whom the present journal issue is dedicated.

The author is greatly indebted to Prof. Wolfgang Pompe for the precious mentoring, fruitful collaboration, and continuous support over the last decade. He would like to thank Prof. Hartmut Worch for many stimulating discussions and encouragements. Acknowledged are long-standing collaborations with A. De Vita, M. Stengel and M. C. Payne. This work has been supported by the Alexander von Humboldt Stiftung and by the Deutsche Forschungsgemeinschaft within the Emmy-Noether Programme (CI 144/2-1). Part of the work has been carried out under the HPC-EUROPA project (RII3-CT-2003-506079), with the support of the European Community - Research Infrastructure Action under the FP6 “Structuring the European Research Area” Programme. The CPU time required to perform the simulations described has been allocated on the HPCx supercomputer facilities through the UKCP consortium, UK, and on the supercomputers at the HLRS, Stuttgart, the SSC, Karlsruhe and the ZIH, Dresden, Germany.

## References

- [1] K. R. Lawless: Rep. Prog. Phys. 37 (1974) 231-316.



- [2] Z. Zhen-Hua, D. Hui-Qiu, L. Wei-Xue, H. Wang-Yu: *Acta Phys. Sin.* 55 (2006) 3157-3164.
- [3] S. Piscanec, L. Colombi Ciacchi, E. Vesselli, G. Comelli, O. Sbaizero, S. Meriani, A. De Vita: *Acta Mater.* 52 (2004) 1237-1245.
- [4] G. Jerkiewicz, G. Vatankhah, J. Lessard, M. P. Soriaga, Y.-S. Park: *Electrochim. Acta* 49 (2004) 1451-1459.
- [5] F. B. Diniz, R. R. Ueta: *Electrochim. Acta* 49 (2004) 4281-4286.
- [6] F. P. Fehlner, in: *Low temperature oxidation*, John Wiley and Sons, New York (1986).
- [7] C. L. Muhlstein, E. A. Stach, R. O. Ritchie: *Acta Mater.* 50 (2002) 3579-3595.
- [8] E. Fromm, in: *Kinetics of metal-gas interactions at low temperatures*, Springer-Verlag, Berlin Heidelberg (1998).
- [9] G. Tamann: *Z. Anorg. Allgem. Chem.* 111 (1920) 78-89.
- [10] N. Cabrera, N. F. Mott: *Rep. Prog. Phys.* 12 (1948) 163-184.
- [11] F. P. Fehlner, N. F. Mott: *Oxid. Met.* 2 (1970) 59-99.
- [12] L. P. H. Jeurgens, W. G. Sloof, F. D. Tichelaar, E. J. Mittemeijer: *J. Appl. Phys.* 92 (2002) 1649-1656.
- [13] F. Reichel, L. P. H. Jeurgens, E. J. Mittemeijer: *Phys. Rev. B* 74 (2006) 144103.
- [14] E. Lundgren, G. Kresse, C. Klein, M. Borg, J. N. Andersen, M. De Santis, Y. Gauthier, C. Konvicka, M. Schmid, P. Varga: *Phys. Rev. Lett.* 88 (2002) 246103.
- [15] R. Benedek, D. N. Seidman, M. Minkoff, L. H. Yang, A. Alavi: *Phys. Rev. B* 60 (1999) 16094-16102.

- [16] S. Köstlmeier-Gemming, C. Elsässer: *Phys. Chem. Chem. Phys.* 3 (2001) 5140-5144.
- [17] M. W. Ruckman, J. Chen, M. Strongin, E. Horache: *Phys. Rev. B* 45 (1992) 14273-14278.
- [18] F. M. Jacobsen, S. Raaen, M. W. Ruckman, M. Strongin: *Phys. Rev. B* 52 (1995) 11339-11342.
- [19] M. C. Payne, M. P. Teter, D. C. Allan, T. A. Arias, J. D. Joannopoulos: *Rev. Mod. Phys.* 64 (1992) 1045-1097.
- [20] J. Hafner: *Acta Mater.* 48 (2000) 71-92.
- [21] K. Reuter, M. Scheffler: *Phys. Rev. Lett.* 90 (2003) 046103.
- [22] M. W. Finnis, A. Y. Lozovoi, A. Alavi: *Annu. Rev. Mater. Res.* 35 (2005) 167-207.
- [23] T. Campbell, R. K. Kalia, A. Nakano, P. Vashishta, S. Ogata, S. Rodgers: *Phys. Rev. Lett.* 82 (1999) 4866-4869.
- [24] P. Vashishta, R. K. Kalia, A. Nakano: *J. Phys. Chem. B* 110 (2006) 3727-3733.
- [25] G. Galli, A. Pasquarello, in: M. P. Allen, D. J. Tildesley (Eds.), *Computer Simulation in Chemical Physics*, Kluwer Academic Publishers, Dordrecht (1993) 261-313.
- [26] D. Marx, J. Hutter, in: J. Grotendorst (Ed.), *Modern Methods and Algorithms of Quantum Chemistry*, John von Neumann Institute of Computing, Jülich (2000) 301-449.
- [27] L. Verlet: *Phys. Rev.* 156 (1967) 98-103.
- [28] A. De Vita, A. Canning, G. Galli, F. Gygi, F. Mauri, R. Car: *EPFL Supercomput. Rev.* 6 (1994) 22.
- [29] R. Car, M. Parrinello: *Phys. Rev. Lett.* 55 (1985) 2471-2474.

- [30] J. P. Perdew, Y. Wang: Phys. Rev. B, 45 (1992) 13244-13249.
- [31] N. Troullier, J. L. Martins: Phys. Rev. B 43 (1991) 1993-2006.
- [32] P. E. Blöchl: Phys. Rev. B 50 (1994) 17953-17979.
- [33] J. VandeVondele, A. De Vita: Phys. Rev. B 60 (1999) 13241-13244.
- [34] M. Stengel, A. De Vita: Phys. Rev. B 62 (2000) 15283-15286.
- [35] L. C. Ciacchi, M. C. Payne: Phys. Rev. Lett. 92 (2004) 176104.
- [36] L. C. Ciacchi, M. C. Payne: Phys. Rev. Lett. 95 (2005) 196101.
- [37] A. D. Becke, K. E. Edgecombe: J. Chem. Phys. 92 (1990) 5397-5403.
- [38] H. Brune, J. Wintterlin, R. J. Behm, G. Ertl: Phys. Rev. Lett 68 (1992) 624-627.
- [39] M. Schmid, G. Leonardelli, R. Tscheließnig, A. Biedermann, P. Varga: Surf. Sci. 478 (2001) L355-L-362.
- [40] A. J. Komrowski, J. Z. Sexton, A. C. Kummel: Phys. Rev. Lett. 87 (2001) 246103.
- [41] J. Wintterlin, R. Schuster, G. Ertl: Phys. Rev. Lett. 77 (1996) 123-126.
- [42] Y. Yourdshahyan, B. Razaznejad, B. I. Lundqvist: Phys. Rev. B 65 (2002) 075416.
- [43] R. F. W. Bader, in: Atoms in Molecules: A Quantum Theory, Oxford University Press, Oxford (1990).
- [44] H. Brune, J. Wintterlin, G. Ertl, J. Wiechers, R. J. Behm: J. Chem. Phys. 99 (1993) 2128-2148.
- [45] P. C. Snijders, L. P. H. Jeurgens, W. G. Sloof: Surf. Sci. 589 (2005) 98-105.
- [46] N. Seriani, W. Pompe, L. C. Ciacchi: J. Phys. Chem. B 110 (2006) 14860-14869.

- [47] F. Esaka, K. Furuya, H. Shimada, M. Imamura, N. Matsubayashi, H. Sato, A. Nishijima, A. Kawana, H. Ichimura, T. Kikuchi: J. Vac. Sci. Technol. A 15 (1997) 2521-2528.
- [48] V. Maurice, G. Despert, S. Zanna, M.-P. Bacos, P. Marcus: Nature Mater. 3 (2004) 687-691.
- [49] M. Lazzeri, A. Selloni: Phys. Rev. Lett. 287 (2001) 266105.
- [50] M. Svetina, L. Colombi Ciacchi, O. Sbaizero, S. Meriani, A. De Vita: Acta Mater. 49 (2001) 2169-2177.
- [51] N. C. Saha, J. Tompkins: J. Appl. Phys. 72 (1992) 3072-3079.
- [52] L. Österlund, I. Zorić, B. Kasemo: Phys. Rev. B 55 (1997) 15452-15455.
- [53] L. P. H. Jeurgens, W. G. Sloof, F. D. Tichelaar, E. J. Mittemeijer: Phys. Rev. B 62 (2000) 4707-4719.
- [54] L. C. Ciacchi, J. Bagdahn, D. J. Cole, M. C. Payne, P. Gumbsch, submitted for publication.

Correspondence address:

Dr. Lucio Colombi Ciacchi

Fraunhofer Institut für Werkstoffmechanik IWM,  
Wöhlerstr. 11, 79098 Freiburg, Germany.

Tel.: +49 761 5142113

Fax: +49 761 5142404

email: lucio@izbs.uni-karlsruhe.de

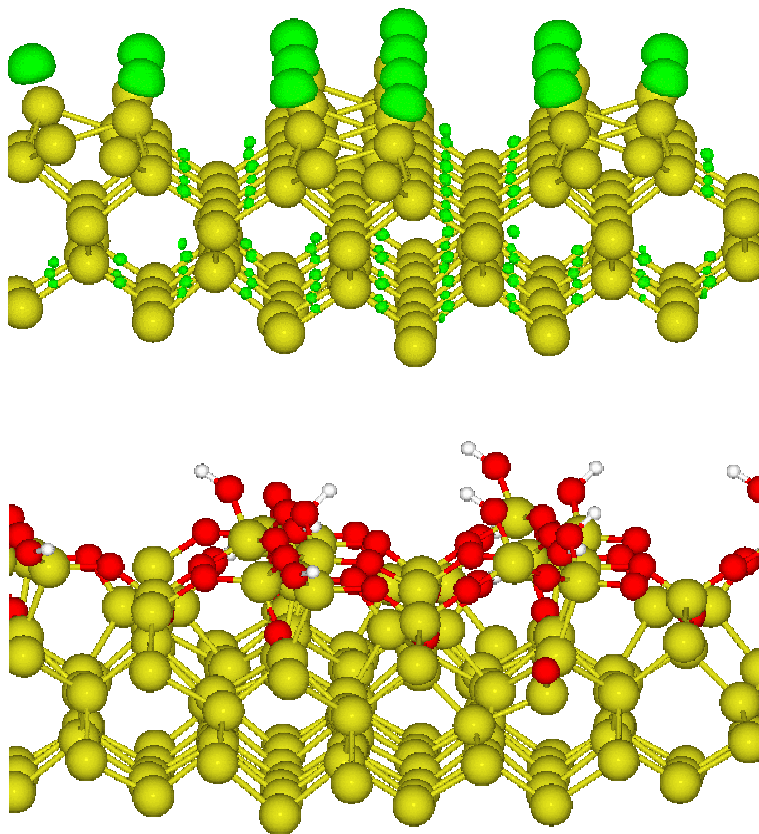


Figure 1: Top: Model of a bare reconstructed Si(001) surface displayed with its computed Electron Localisation Function (green isosurface) showing the presence of reactive dangling bonds on exposed Si atoms. Bottom: model of an oxidised and hydroxylated Si(001) surface as obtained in a series of FPMD simulations [36, 54].

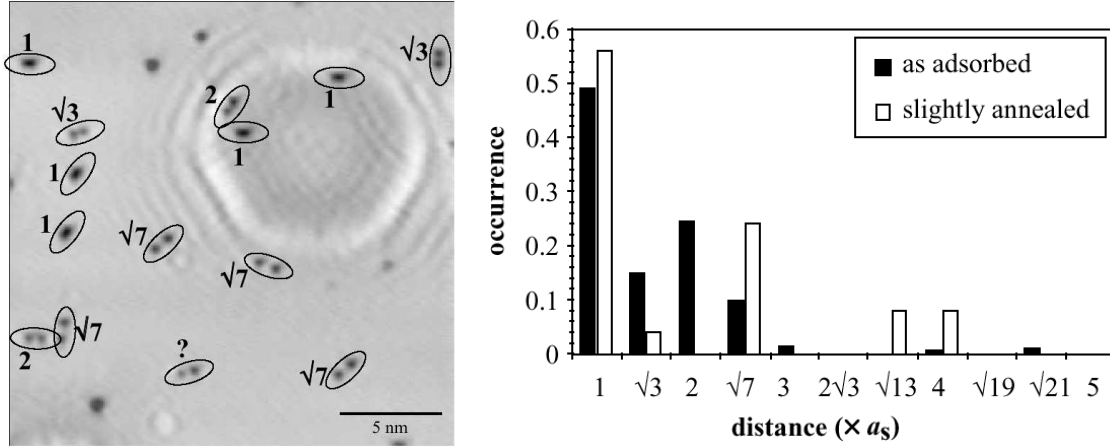


Figure 2: Left: STM image of a bare Al(111) surface upon exposure to an oxygen gas at 150 K. Distances between pairs of oxygen atoms are indicated in units of the Al–Al nearest neighbour distance. Right: Histogram showing the relative number of atom pairs separated by the Al–Al distances reported on the abscissa. The dark spots and the histogram line indicated with “1” are in fact associated with isolated oxygen atoms produced via non-adiabatic abstractive adsorption processes [40]. (Reproduced with permission from Ref. [39], copyright Elsevier 2001).

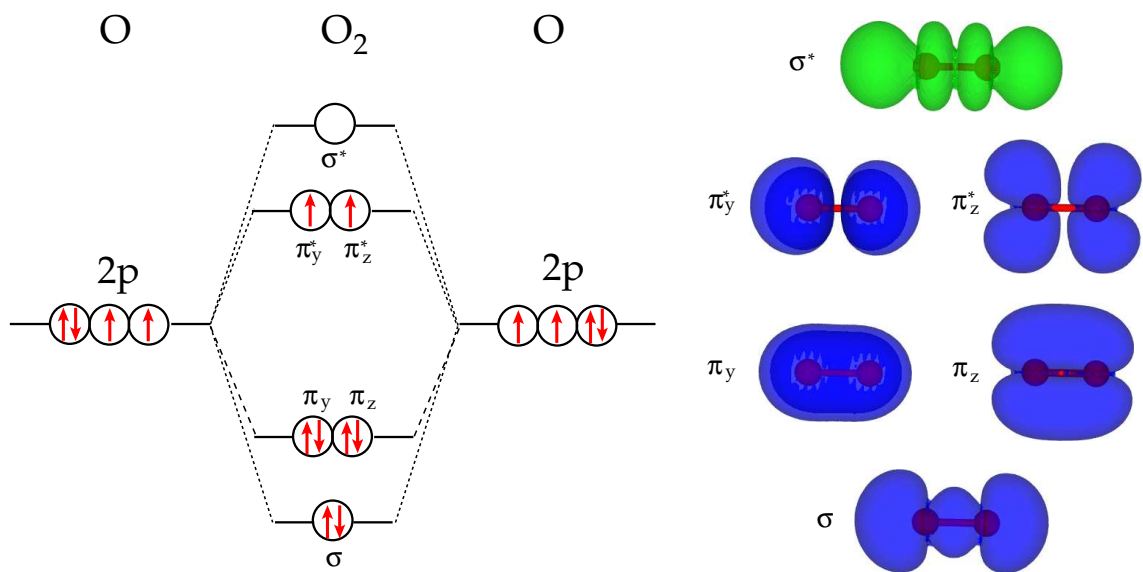


Figure 3: Scheme of the valence molecular orbitals of  $O_2$  (left) in its ground state and their corresponding associated particle densities (right) represented as blue and green isosurfaces for filled and empty orbitals, respectively.

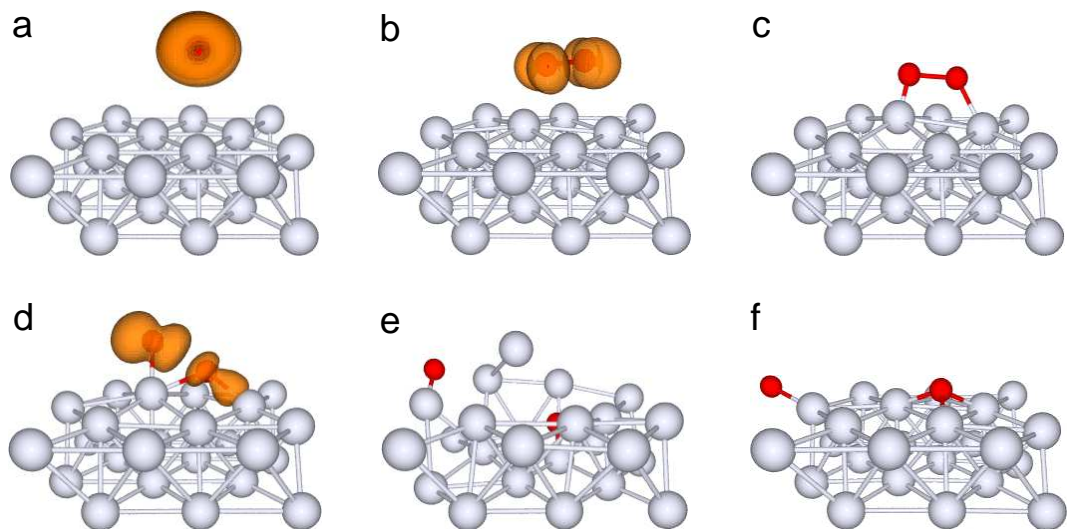


Figure 4: Snapshots from a FPMD simulation of the adsorption of a dioxygen molecule on the Al(111) surface [35]. The spin-density of the system is represented as an orange isosurface. Note the partial filling of the  $\sigma^*$  antibonding orbital (snapshot d) which triggers the “hot-atom” dissociation event.



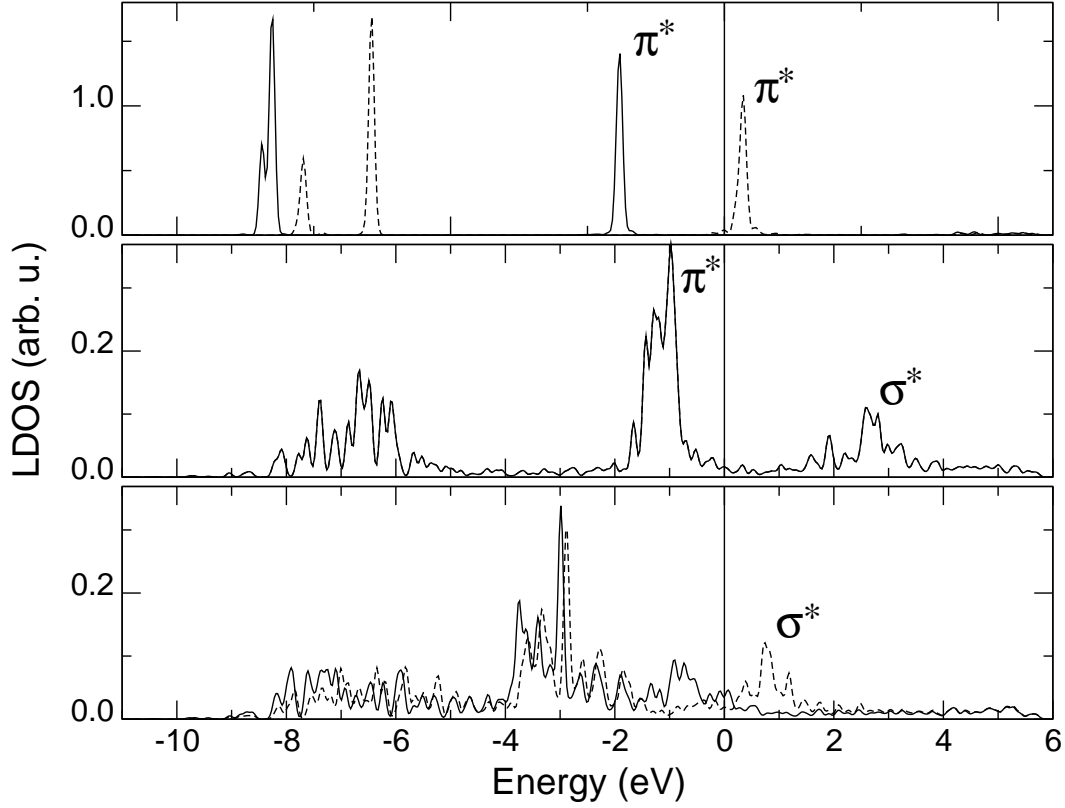


Figure 5: Evolution of the computed local density of states (LDOS) projected onto the O atoms during the adsorption of an  $\text{O}_2$  molecule on the Al(111) surface. The continuous and dashed lines correspond to the majority and minority spin manifolds, respectively, and the Fermi level is indicated with a vertical line. From top to bottom, the graphs refer to an oxygen molecule far from the surface, adsorbed on the surface (filling of the  $\pi^*$  orbitals and spin-quenching), and at the initial moment of dissociation (partial filling of the  $\sigma^*$  orbital).

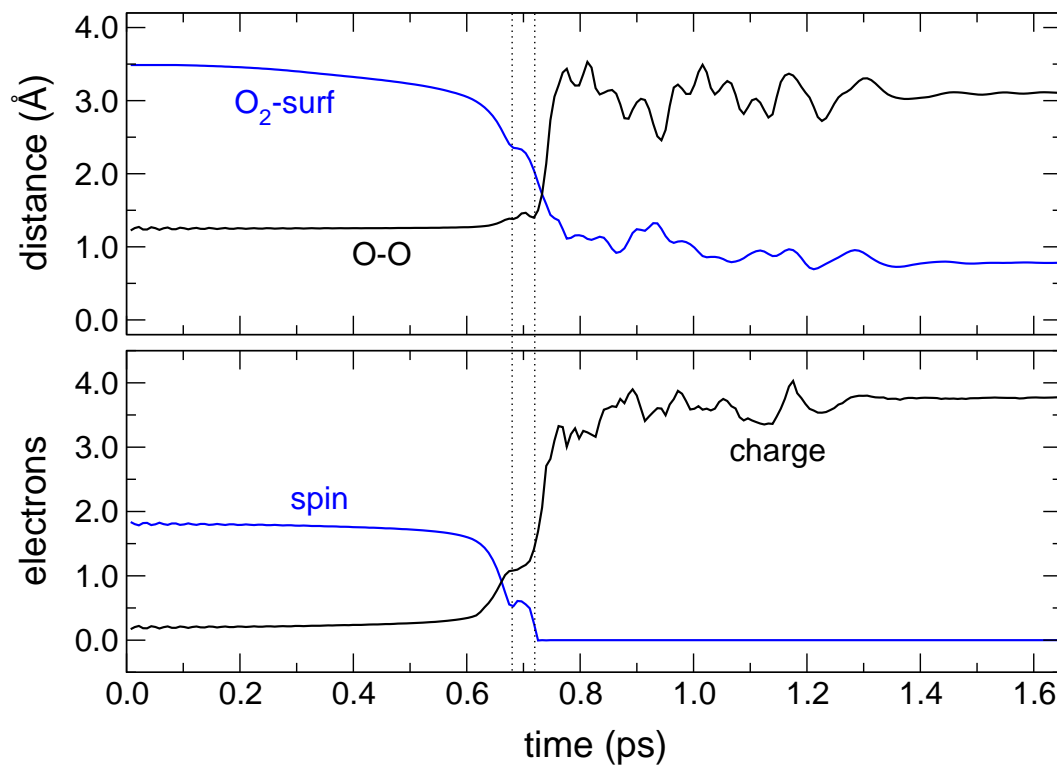


Figure 6: Dynamics of an  $\text{O}_2$  molecule adsorbing dissociatively on the  $\text{Al}(100)$  surface simulated by FPMD. Top graph: evolution of the O–O distance and of the height of the centre of mass of the O atoms with respect to the average height of the surface Al atoms. Bottom graph: evolution of the spin-density and of the atomic charge integrated within the Bader regions associated with both O atoms.

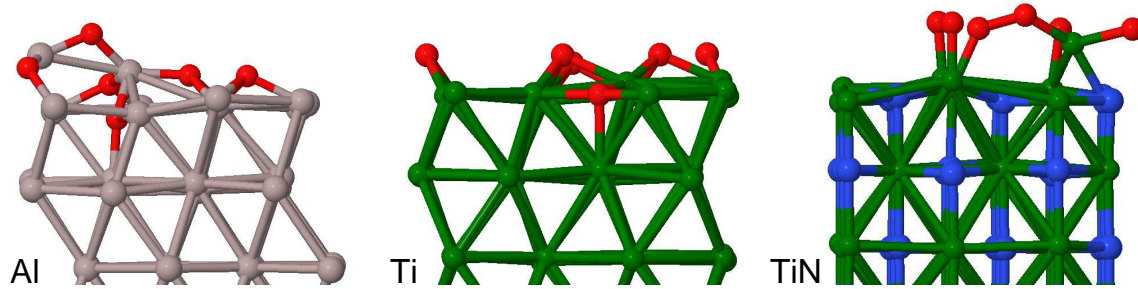


Figure 7: Structures of partially oxidised metal surfaces as obtained in FPMD simulations (only the three topmost metal layers are shown, for clarity). The oxygen atom coverage of the surfaces is 0.5 in the case of Al(111) and Ti(111) and 0.67 in the case of TiN(001). Note the spontaneous incorporation of O atoms underneath the surface in the case of Al and Ti, the extraction of metal atoms from the surface layer in the case of Al and TiN, and the presence of an adsorbed  $O_2$  molecule on TiN.

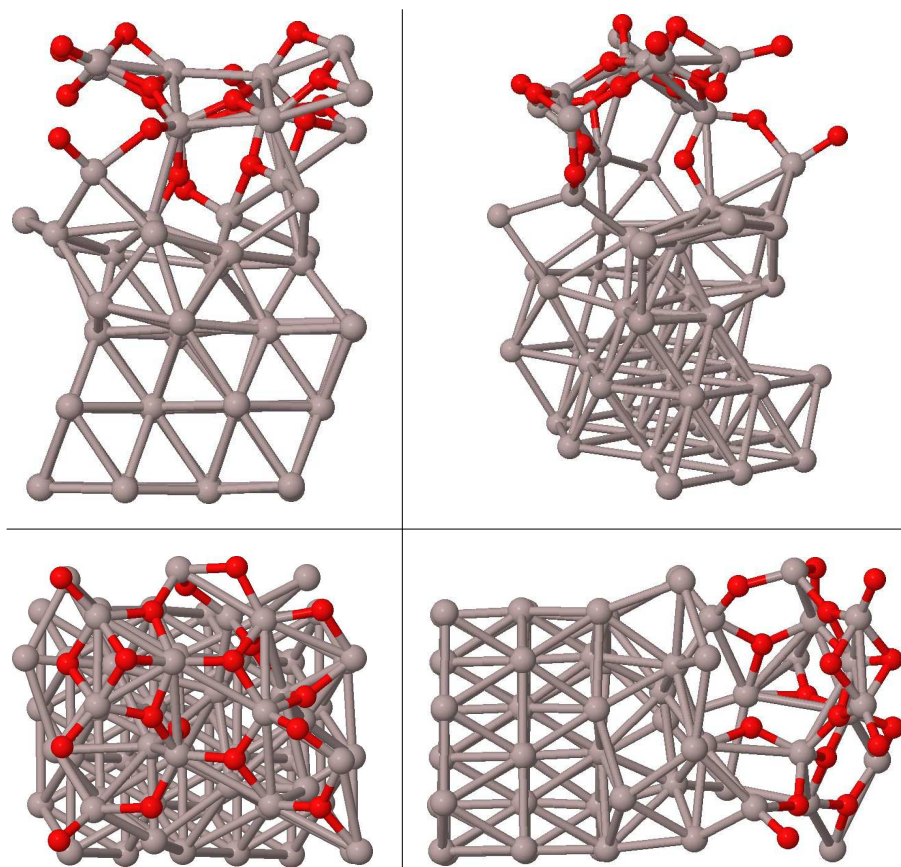


Figure 8: Model of a native oxide layer grown on the Al(111) surface (the oxygen coverage is 1.5 ML), as obtained in a series of FPMD simulations. Orthogonal projections and perspective view (top right).

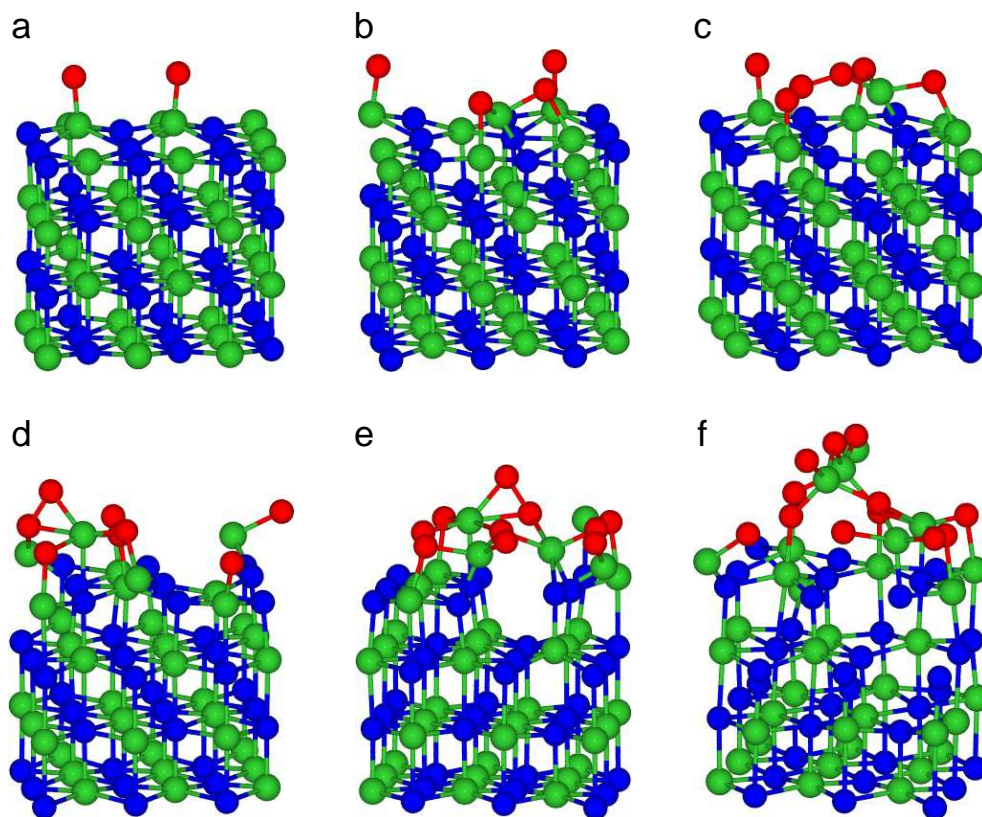


Figure 9: Final snapshots of consecutive FPMD simulations of the initial oxide formation on the TiN(001) surface. The oxygen coverage increases from (a) 0.22 ML to (f) 1.33 ML.

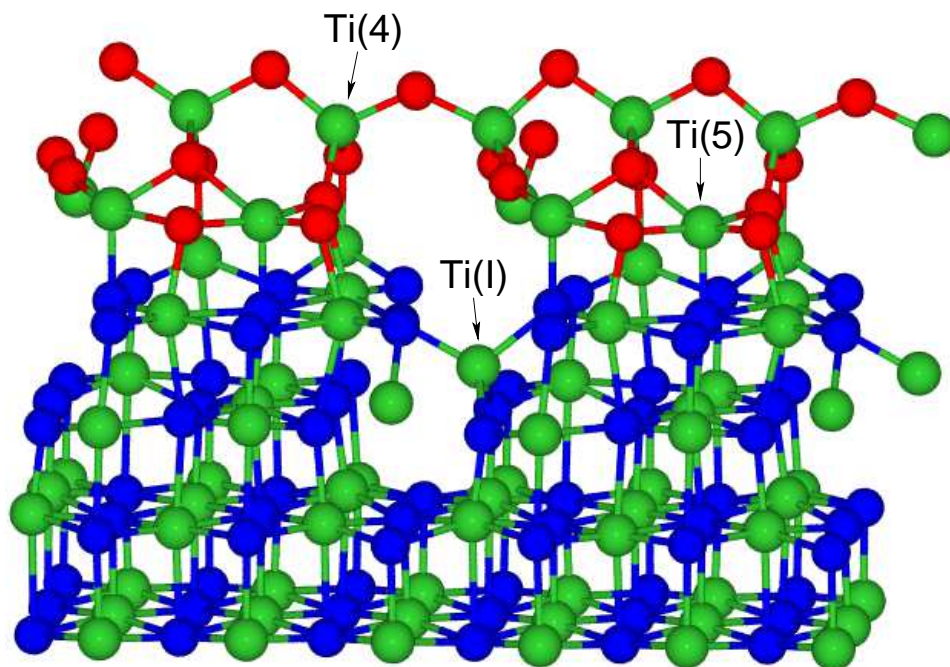


Figure 10: Model of a native oxide layer grown on the TiN(001) surface (the oxygen coverage is 1.33 ML), as obtained in a series of FPMD simulations. A fourfold-coordinated Ti atom is indicated with Ti(4), a fivefold-coordinated Ti atom with Ti(5), and an atom in interstitial position with respect to the TiN lattice with Ti(I).